

Large transverse momentum dilepton and photon production by photoproduction processes^{*}

FU Yong-Ping(傅永平)¹⁾ LI Yun-De(李云德)²⁾

Department of Physics, Yunnan University, Kunming 650091, China

Abstract: We calculate the production of large transverse momentum dileptons and photons by using direct and resolved photoproduction processes in relativistic heavy ion collisions. Considering the central collisions of heavy nuclei at Relativistic Heavy Ion Collider (RHIC) and Large Hadron Collider (LHC) energies, we find that the photoproduction processes modify the dilepton and photon production in the large transverse momentum region.

Key words: photoproduction, dilepton production, photon production

PACS: 12.38.Bx, 12.39.St, 13.85.Qk **DOI:** 10.1088/1674-1137/36/8/007

1 Introduction

Real photons and dileptons are considered to be a useful probe for the investigation of strongly-interacting media due to their very long mean free path. One of the important goals in the study of relativistic heavy ion collisions is to identify various sources for producing the electromagnetic information. The photons (virtual photons) are produced from various processes in relativistic heavy ion collisions. These sources include primary hard photons from initial parton collisions [1–8], thermal photons from the quark-gluon plasma (QGP) [9–18], hadronic gas [19–21], jet-photon conversion [22–25], and photons from hadronic decays after freeze-out [26]. The parton collisions are a well-known source of large transverse momentum (P_T) photons (virtual photons).

In this paper we study the production of large P_T dileptons and photons produced by photoproduction processes in relativistic heavy ion collisions. The photoproduction processes play a fundamental role in the ep deep-inelastic scattering at the Hadron-Electron Ring Accelerator (HERA)($\sqrt{s} = 300$ GeV) [27–29]. We extend the photoproduction mechanism to the relativistic heavy ion collisions. A high energy photon

emitted from the incident electron directly interacts with the proton by the interaction of the $\gamma p \rightarrow$ jets in the ep deep-inelastic scattering. Charged partons of the colliding nucleons can also emit high energy photons and resolved photons. Then these photons (resolved photons) interact with the partons of other nucleons in relativistic heavy ion collisions [30–32].

2 Photoproduction

In direct photoproduction processes, the high energy photon emitted from the charged parton of the incident nucleon interacts with the parton of another incident nucleon by the interaction of $q\gamma \rightarrow q\gamma^*$ (γ) [32]. A virtual photon can decay into a lepton pair, therefore the cross section of the production of large P_T dileptons can be written as [3]

$$\frac{d\sigma_{AB \rightarrow l^+l^-X}}{dM^2 dP_T^2 dy} = \frac{\alpha}{3M^2} \sqrt{1 - \frac{4m_l^2}{M^2}} \left(1 + \frac{2m_l^2}{M^2} \right) \times E_{\gamma^*} \frac{d\sigma_{AB \rightarrow \gamma^* X}}{d^3P}, \quad (1)$$

where the term $\sqrt{1 - 4m_l^2/M^2}$ represents the mass threshold for producing the dilepton, m_l is the lepton mass, and M is the invariant mass of the lepton pair.

Received 1 November 2011, Revised 9 December 2011

^{*} Supported by National Natural Science Foundation of China (10665003, 11065010)

1) E-mail: yunfyp@sina.cn

2) E-mail: yndxlyd@163.com

©2012 Chinese Physical Society and the Institute of High Energy Physics of the Chinese Academy of Sciences and the Institute of Modern Physics of the Chinese Academy of Sciences and IOP Publishing Ltd

The cross section of large P_T virtual photons produced by direct photoproduction processes (dir. pho.) in hadronic collisions ($AB \rightarrow \gamma^* X$) is given by

$$E_{\gamma^*} \frac{d\sigma_{\text{dir.pho.}}}{d^3P} = \frac{2}{\pi} \int dx_a \int dx_b G_{a/A}(x_a, Q^2) \times G_{b/B}(x_b, Q^2) f_{\gamma/q_a}(z_a) \frac{x_a x_b z_a}{x_a x_b - x_a x_2} \times \frac{d\hat{\sigma}}{d\hat{t}}(x_a, x_b, z_a, P_T, M^2), \quad (2)$$

where $G_{a/A}(x_a, Q^2)$ and $G_{b/B}(x_b, Q^2)$ are the parton distributions of nucleons, $f_{\gamma/q_a}(z_a)$ is the photon spectrum from the quark, x_a and x_b are the momentum fractions of the partons. Here the square of the center-of-mass energy for the subprocess is $\hat{s} = x_a x_b z_a s_{NN}$. The momentum fraction z_a of the photon emitted from the quark is

$$z_a = \frac{x_b x_1 - \tau}{x_a x_b - x_a x_2}, \quad (3)$$

where

$$x_1 = \frac{1}{2}(x_T^2 + 4\tau)^{1/2} e^y, \quad (4)$$

and

$$x_2 = \frac{1}{2}(x_T^2 + 4\tau)^{1/2} e^{-y}, \quad (5)$$

here $x_T = 2P_T/\sqrt{s_{NN}}$, $\tau = M^2/s_{NN}$. $\sqrt{s_{NN}}$ is the energy in the center-of-mass system. y is the rapidity of the system. In this paper, we choose the mass range as $100 \text{ MeV} \leq M \leq 300 \text{ MeV}$. The subscript $a(b)$ denotes the parton of the nucleon $A(B)$. The parton a of the incident nucleon A can emit a large P_T photon, then the high energy photon interacts with the parton b of another incident nucleon B by the interaction of $q_b \gamma \rightarrow q(\gamma^* \rightarrow l^+ l^-)$.

The photon spectrum from the charged parton can be expressed as [30–32]

$$f_{\gamma/q}(z) = e_q^2 \frac{\alpha}{2\pi} \frac{1 + (1-z)^2}{z} \ln\left(\frac{Q_1^2}{Q_2^2}\right), \quad (6)$$

where e_q is the charge of the quark, α is the electromagnetic coupling parameter, and z is the momentum fraction of the photon emitted from the charged parton. The values $Q_1^2 = \hat{s}/4 - m_l^2$ and $Q_2^2 = 1 \text{ GeV}^2$ stand for the maximum and minimum values of the momentum transfer, respectively. Here \hat{s} is the square of the center-of-mass energy for the subprocess. Although the photoproduction process contains higher-order QED coupling parameters, the photon spectrum from the quark may enhance its contribution. The photon spectrum from the quark depends on the collision energy $\sqrt{s_{NN}}$. We express the photon spectrum as $f_{\gamma/q}(z) \propto \ln((\hat{s}/4 - m_l^2)/1 \text{ GeV}^2) =$

$\ln(\sqrt{s_{NN}}/1 \text{ GeV})^2 + \ln(x_a x_b z_a \cdots / 4 - m_l^2/s_{NN})$, where $\hat{s} = x_a x_b z_a s_{NN}$ for direct photoproduction processes and $\hat{s} = x_a x_b z_a z_{a'} s_{NN}$ for resolved photoproduction processes. Since the collision energy at the RHIC ($\sqrt{s_{NN}}=200 \text{ GeV}$) and the LHC ($\sqrt{s_{NN}}=5500 \text{ GeV}$) is large, the photon spectrum from the quark may be important in the photoproduction processes of the relativistic heavy ion collisions.

The QED Compton process $q\gamma \rightarrow q\gamma^*$ can be obtained by the following ratio [2]

$$\frac{d\hat{\sigma}/d\hat{t}(q\gamma \rightarrow q\gamma^*)}{d\hat{\sigma}/d\hat{t}(qg \rightarrow q\gamma^*)} = 6 \frac{\alpha}{\alpha_s} e_q^2, \quad (7)$$

and we have

$$\frac{d\hat{\sigma}}{d\hat{t}}(q\gamma \rightarrow q\gamma^*) = \frac{\pi\alpha^2 e_q^4}{\hat{s}^2} 2 \left(-\frac{\hat{t}}{\hat{s}} - \frac{\hat{s}}{\hat{t}} - \frac{2M^2 \hat{u}}{\hat{s}\hat{t}} \right), \quad (8)$$

where the Mandelstam variables are $\hat{s} = x_a x_b z_a s_{NN}$, $\hat{u} = M^2 - x_b x_1 s_{NN}$ and $\hat{t} = M^2 - x_a x_2 z_a s_{NN}$.

The parton distribution $G(x, Q^2)$ of the nucleon is [6]

$$G(x, Q^2) = R(x, Q^2) [Zp(x, Q^2) + Nn(x, Q^2)] / A, \quad (9)$$

where $R(x, Q^2)$ is the nuclear modification of the structure function [7], Z is the proton number, N is the neutron number and A is the nucleon number. $p(x, Q^2)$ and $n(x, Q^2)$ are the parton distributions of the proton and neutron, respectively. Since protons and neutrons have different numbers of up and down valence quarks, the isospin effect of nucleons can be expressed by the sum of the parton distributions of the proton and neutron.

If the parton a of the incident nucleon A emits a resolved photon, the parton a' of the resolved photon interacts with the parton b of another incident nucleon B by the interactions of $q_{a'} \bar{q}_b \rightarrow g\gamma^*$, $q_{a'} g_b \rightarrow q\gamma^*$ and $q_b g_{a'} \rightarrow q\gamma^*$ [32]. The cross section of large P_T virtual photons produced by resolved photoproduction processes (res. pho.) is given by

$$E_{\gamma^*} \frac{d\sigma_{\text{res.pho.}}}{d^3P} = \frac{2}{\pi} \int dx_a \int dx_b \int dz_{a'} G_{a/A}(x_a, Q^2) \times G_{b/B}(x_b, Q^2) f_{\gamma/q_a}(z_a) \times G_{q_{a'}/\gamma}(z_{a'}, Q^2) \frac{x_a x_b z_a z_{a'}}{x_a x_b z_{a'} - x_a z_{a'} x_2} \times \frac{d\hat{\sigma}}{d\hat{t}}(x_a, x_b, z_a, z_{a'}, P_T, M^2), \quad (10)$$

where $G_{q_{a'}/\gamma}(z_{a'}, Q^2)$ is the parton distribution of the resolved photon [8]. Here the variable z_a is

$$z_a = \frac{x_b x_1 - \tau}{x_a x_b z_{a'} - x_a z_{a'} x_2}. \quad (11)$$

The subprocesses of resolved photoproduction processes of the annihilation and Compton scattering are given by [2]

$$\frac{d\hat{\sigma}}{d\hat{t}}(q\bar{q} \rightarrow g\gamma^*) = \frac{\pi\alpha_s\alpha_s e_q^2}{\hat{s}^2} \frac{8}{9} \left(\frac{\hat{u}}{\hat{t}} + \frac{\hat{t}}{\hat{u}} + \frac{2M^2\hat{s}}{\hat{t}\hat{u}} \right), \quad (12)$$

and

$$\frac{d\hat{\sigma}}{d\hat{t}}(qg \rightarrow q\gamma^*) = \frac{\pi\alpha_s\alpha_s e_q^2}{\hat{s}^2} \frac{1}{3} \left(-\frac{\hat{t}}{\hat{s}} - \frac{\hat{s}}{\hat{t}} - \frac{2M^2\hat{u}}{\hat{s}\hat{t}} \right). \quad (13)$$

The Mandelstam variables in resolved photoproduction processes are $\hat{s} = x_a x_b z_a z_{a'} s_{NN}$, $\hat{u} = M^2 - x_b x_1 s_{NN}$ and $\hat{t} = M^2 - x_a x_2 z_a z_{a'} s_{NN}$. The strong coupling constant is given by

$$\alpha_s = \frac{12\pi}{(33 - 2N_f) \ln(Q^2/\Lambda^2)}, \quad (14)$$

where N_f is the number of quark flavors and Λ is the QCD scale parameter. We choose the momentum scales as $Q^2 = 4P_T^2$ and $\Lambda = 0.2$ GeV.

The categories of real photons with large P_T are similar to the cases of the dilepton production. The cross sections of real photons can be derived from the cross sections of the dilepton production if $M^2 = 0$. Now the maximum momentum transfer Q_1^2 is $\hat{s}/4$ in the real photon production.

The cross section of real photons produced by direct photoproduction processes is given by the following

$$E_\gamma \frac{d\sigma_{\text{dir.pho.}}}{d^3P} = \frac{2}{\pi} \int dx_a \int dx_b G_{a/A}(x_a, Q^2) \times G_{b/B}(x_b, Q^2) f_{\gamma/q_a}(z_a) \frac{x_a x_b z_a}{x_a x_b - x_a x_2} \times \frac{d\hat{\sigma}}{d\hat{t}}(q\gamma \rightarrow q\gamma, x_a, x_b, z_a, P_T), \quad (15)$$

where the cross section $d\hat{\sigma}/d\hat{t}(q\gamma \rightarrow q\gamma)$ is derived from Eq. (8) (but with $M^2 = 0$). The real photon production induced by resolved photoproduction processes is

$$E_\gamma \frac{d\sigma_{\text{res.pho.}}}{d^3P} = \frac{2}{\pi} \int dx_a \int dx_b \int dz_{a'} G_{a/A}(x_a, Q^2) \times G_{b/B}(x_b, Q^2) f_{\gamma/q_a}(z_a) \times G_{q_{a'}/\gamma}(z_{a'}, Q^2) \frac{x_a x_b z_a z_{a'}}{x_a x_b z_{a'} - x_a z_{a'} x_2} \times \frac{d\hat{\sigma}}{d\hat{t}}(x_a, x_b, z_a, z_{a'}, P_T), \quad (16)$$

where the subprocesses are similar to the cases in Eqs. (12) and (13) (but with $M^2 = 0$).

3 Other production sources

In the first stage of relativistic heavy ion collisions, the prompt photons (virtual photons) are those produced by Compton scattering $qg \rightarrow q\gamma$ (or $\gamma^* \rightarrow l^+l^-$), annihilation of two partons $q\bar{q} \rightarrow g\gamma$ (or $\gamma^* \rightarrow l^+l^-$), and bremsstrahlung emitted from final state partons $ab \rightarrow (c \rightarrow x\gamma$ (or $\gamma^* \rightarrow l^+l^-$))d [1–3, 13]. The initial parton collisions are the main source of hard photon (virtual photon) production [3–5].

In the QGP phase, thermal photons are also produced by Compton scattering $q_{\text{th}}g_{\text{th}} \rightarrow q_{\text{th}}\gamma$ and annihilation $q_{\text{th}}\bar{q}_{\text{th}} \rightarrow g_{\text{th}}\gamma$ of thermal partons [10, 11]. The leading order production of thermal dileptons with the low invariant mass and transverse momentum are produced by $q_{\text{th}}\bar{q}_{\text{th}} \rightarrow \gamma^* \rightarrow l^+l^-$ [9, 12].

The jet-photon conversion is induced by Compton scattering ($q_{\text{th}}g_{\text{jet}}$ (or $q_{\text{jet}}g_{\text{th}}$) $\rightarrow q\gamma$) and annihilation ($q_{\text{jet}}\bar{q}_{\text{th}}$ (or $q_{\text{th}}\bar{q}_{\text{jet}}$) $\rightarrow g\gamma$) of jets passing through the thermal medium. The contribution of jet-photon conversion is also important in the large P_T region [22, 23]. However, the spectrum of dileptons produced by jet-dilepton conversion ($q_{\text{jet}}\bar{q}_{\text{th}}$ (or $q_{\text{th}}\bar{q}_{\text{jet}}$) $\rightarrow \gamma^* \rightarrow l^+l^-$) falls off with the transverse momentum of dileptons faster than the spectrum of primary hard dileptons in the large P_T region [24, 25].

The background photons and dileptons are those produced from hadronic phase (hadronic reactions) [19–21] and the stage of freeze-out (radiative decays of resonance states) [26]. The background spectrum of hadronic decays ($\pi^0 \rightarrow \gamma\gamma$, $\eta \rightarrow \gamma\gamma$ etc.) can be subtracted from the inclusive photon spectrum by using the statistical techniques of mixed-events in experiments [15]. All the thermal electromagnetic information of QGP phase and hadronic phase are low P_T spectra. It is a challenge to identify the thermal information of the QGP phase from the hadronic phase [12].

4 Numerical results

From Figs. 1–4 we plot the contribution of direct and resolved photoproduction processes at RHIC and LHC energies. The direct and resolved photoproduction processes modify the dilepton spectra in the region of $P_T > 1$ GeV at the RHIC and $P_T > 4$ GeV at the LHC (the panel b of Figs. 1 and 2). The contribution of real photons produced by direct and resolved photoproduction processes is in the region of $P_T > 3$ GeV at the RHIC and $P_T > 7$ GeV at the LHC (the panel b of Figs. 3 and 4). The modification

is not prominent at RHIC energies, but the contribution of photoproduction processes becomes evident in the large P_T region at LHC energies.

Since the thermal information is dominant in the low P_T region, the contribution of thermal dileptons and photons is also calculated. The initial temperature of the QGP is chosen as $T_0 = 370$ MeV at the RHIC and $T_0 = 845$ MeV at the LHC.

The spectra of the jet-dilepton conversion drop rapidly with the transverse momentum of dileptons due to the attenuation function [25, 32] (the panel a of Figs. 1 and 2). Since the rate of the jet-photon conversion is $R_{\text{jet-QGP}} \propto f_{\text{jet}}$, the spectra of the jet-photon conversion do not fall off quickly with the transverse momentum [22, 23] (the panel a of Figs. 3 and 4).

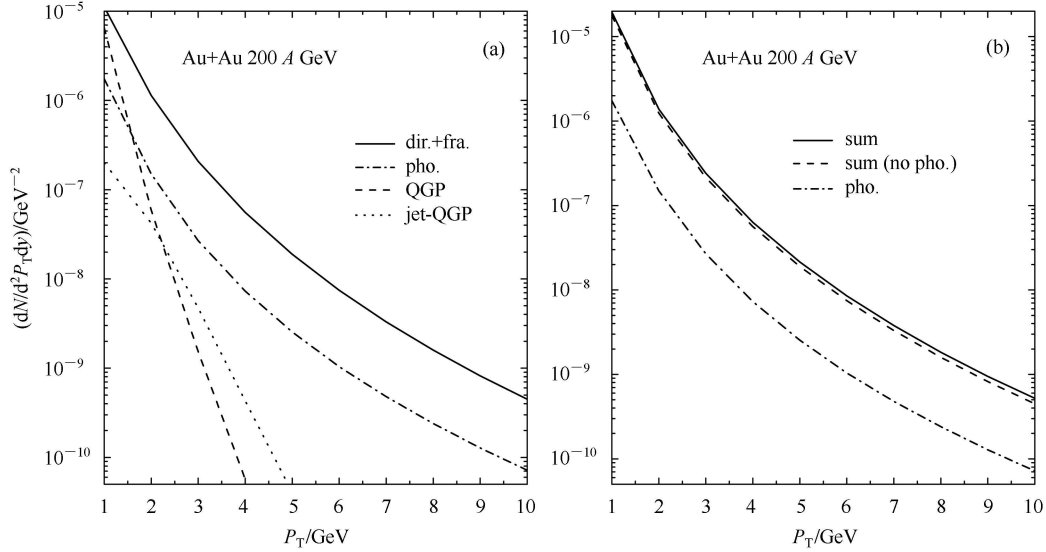


Fig. 1. (a) The production of large P_T dileptons at RHIC energies. Direct dileptons (dir.) are produced by $q\bar{q} \rightarrow q_l^{+1}l^{-}$ and $q\bar{q} \rightarrow g_l^{+1}l^{-}$; fragmentation dileptons (fra.) are produced by $ab \rightarrow (c \rightarrow x_l^{+1}l^{-})d$; pho. denotes direct (dir. pho.) and resolved (res. pho.) photoproduction processes. (b) The contribution of direct and resolved photoproduction processes at RHIC energies. The dashed line is the sum of direct dileptons, fragmentation dileptons, thermal dileptons and jet-dilepton conversions. The solid line is the sum of direct dileptons, fragmentation dileptons, thermal dileptons, jet-dilepton conversions, and dileptons produced by direct and resolved photoproduction processes.

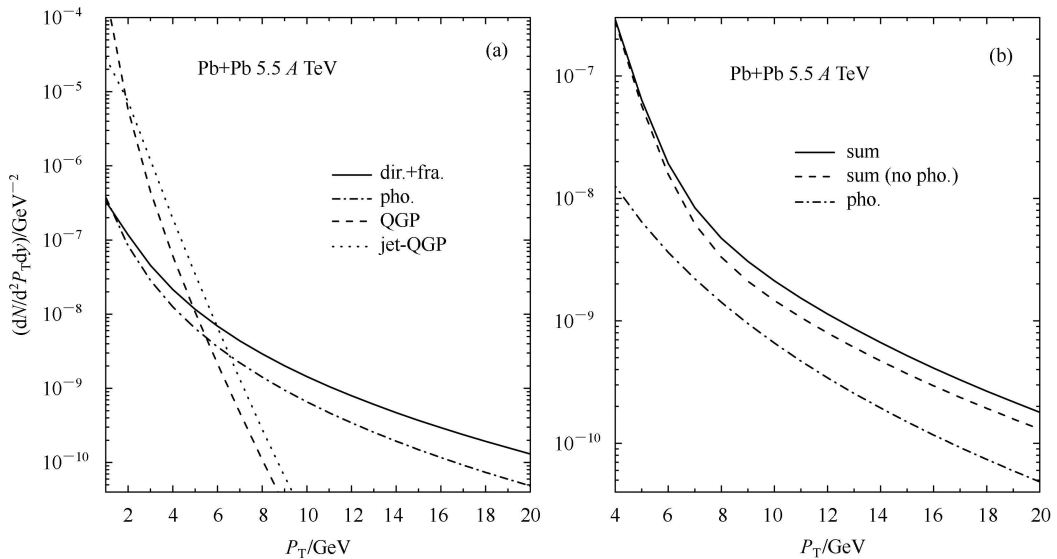


Fig. 2. The same as Fig. 1 but for Pb+Pb collisions at the LHC.

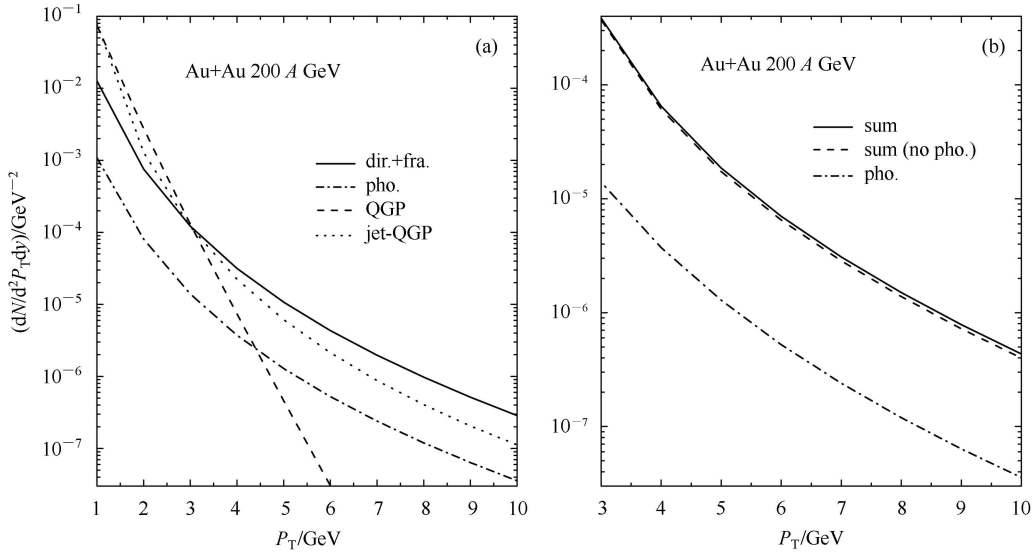


Fig. 3. (a) The production of large P_T photons at RHIC energies. Direct photons (dir.) are produced by $qg \rightarrow q\gamma$ and $q\bar{q} \rightarrow g\gamma$; fragmentation photons (fra.) are produced by $ab \rightarrow (c \rightarrow x\gamma)d$. (b) The contribution of photoproduction processes at RHIC energies. The dashed line is the sum of direct photons, fragmentation photons, thermal photons, and jet-photon conversions. The solid line is the sum of direct photons, fragmentation photons, thermal photons, jet-photon conversions, and photons produced by photoproduction processes.

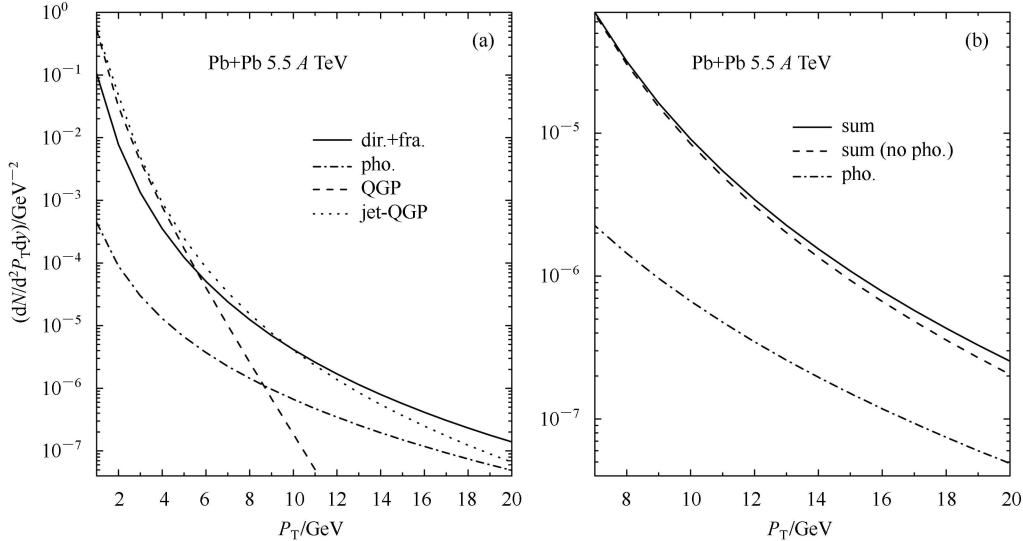


Fig. 4. The same as Fig.3 but for Pb+Pb collisions at LHC energy

Jets passing through the QGP will lose energy. Induced gluon bremsstrahlung, rather than elastic scattering of partons, is the dominant mechanism of the jet energy loss [13, 22, 23, 33, 34]. Based on the AMY formalism, the energy loss of the final state partons can be described as a dependence of the final state parton spectrum dN_{jet}/dE on time [13, 35]. Besides, the energy loss of jets can be scaled as the square of

the distance traveled through the medium [36]. Jets travel only a short distance through the plasma before the jet-photon (or virtual photon) conversion, and do not lose a significant amount of energy. The energy loss effect of jets before they convert into photons (or virtual photons) is found to be small, about 20% [13, 22, 23]. We consider the effective energy loss of jets in the calculation.

5 Conclusion

We study the large P_T dilepton and photon production in relativistic heavy ion collisions induced by photoproduction processes. In the direct photoproduction, the charged parton of the incident nucleon

emits a large P_T photon, then the high energy photon interacts with the parton of another incident nucleon. If the photon emitted from the charged parton is resolved, the parton of the resolved photon can interact with the parton of the nucleon. Our numerical results show that the photoproduction is not prominent at the RHIC, but becomes evident in the large P_T region at the LHC.

References

- 1 Owens J F. Rev. Mod. Phys., 1987, **59**: 465
- 2 Field R D. Applications of Perturbative QCD. Addison-Wesley Publishing Company, 1989
- 3 KANG Z, OIU J, Vogelsang W. Phys. Rev. D, 2009, **79**: 054007
- 4 KANG Z, OIU J, Vogelsang W. Nucl. Phys. A, 2009, **830**: 571
- 5 FU Y P, LI Y D. Chin. Phys. C (HEP & NP), 2010, **34**: 186; FU Y P, LI Y D. Chin. Phys. Lett., 2009, **26**: 111201
- 6 Glück M, Reya E, Vogt A. Z. Phys. C, 1992, **53**: 127
- 7 Eskola K J, Kolhinen V J, Salgado C A. Eur. Phys. J. C, 1999, **9**: 61; Eskola K J, Kolhinen V J, Ruuskanen P V. Nucl. Phys. B, 1998, **535**: 351
- 8 Glück M, Reya E, Vogt A. Phys. Rev. D, 1992, **46**: 1973
- 9 Kajantie K, Kapusta J, McLerran L, Mekjian A. Phys. Rev. D, 1986, **34**: 2746
- 10 Kapusta J, Lichard P, Seibert D. Phys. Rev. D, 1991, **44**: 2774
- 11 WONG C Y. Introduction to High Energy Heavy-Ion Collisions. Singapore: World Scientific, 1994
- 12 Nayak J K, Alam J, Sarkar S, Sinha B. Phys. Rev. C, 2008, **78**: 034903
- 13 Turbide S, Gale C, Jeon S, Moore G D. Phys. Rev. C, 2005, **72**: 014906
- 14 Shuryak E, XIONG L. Phys. Rev. Lett., 1993, **70**: 2241
- 15 Srivastava D K, Gale C et al. Phys. Rev. C, 2003, **67**: 034903
- 16 Pisarski R D. Phys. Lett. B, 1982, **110**: 155
- 17 Shuryak E V, Zahed I. Phys. Rev. C, 2004, **70**: 021901
- 18 Rapp R, Shuryak E. Phys. Lett. B, 2000, **473**: 13
- 19 Turbide S, Rapp R, Gale C. Phys. Rev. C, 2004, **69**: 014903
- 20 Hung C M, Shuryak E V. Phys. Rev. C, 1997, **56**: 453
- 21 Peitzmann T, Thoma M H. Phys. Rep., 2002, **364**: 175
- 22 Fries R J, Müller B, Srivastava D K. Phys. Rev. Lett., 2003, **90**: 132301
- 23 Fries R J, Müller B, Srivastava D K. Phys. Rev. C, 2005, **72**: 041902
- 24 Turbide S, Cale C, Srivastava D K, Fries R J. Phys. Rev. C, 2006, **74**: 014903
- 25 FU Y P, LI Y D. Nucl. Phys. A, 2011, **865**: 76; FU Y P, LI Y D. Chin. Phys. Lett., 2010, **27**: 101202
- 26 Bratkovskaya E L, Cassing W. Nucl. Phys. A, 1997, **619**: 413
- 27 Nisius R. Phys. Rep., 2000, **332**: 165
- 28 Krawczyk M, Zembrzusi A, Staszal M. Phys. Rep., 2001, **345**: 265
- 29 Forshaw J R. hep-ph/9706319.
- 30 Baur G. J. Phys. G, 1998, **24**: 1657
- 31 Drees M, Godbole R M, Nowakowski M, Rindani S D. Phys. Rev. D, 1994, **50**: 2335
- 32 FU Y P, LI Y D. Phys. Rev. C, 2011, **84**: 044906; FU Y P, LI Y D. Chin. Phys. C (HEP & NP), 2011, **35**: 109
- 33 Gyulassy M, Plümer M. Phys. Lett. B, 1990, **243**: 432
- 34 WANG X N, Gyulassy M, Plümer M. Phys. Rev. D, 1995, **51**: 3436
- 35 Arnold P, Moore G D, Yaffe L. J. High Energy Phys., 2001, **11**: 057
- 36 Baier R et al. Nucl. Phys. B, 1997, **484**: 265